

An Ionic Polymer Metal Composite (IPMC)-Driven Linear Peristaltic Microfluidic Pump

Sideris, Eva Ann; De Lange, Hendrik Cornelis; Hunt, Andres

DOI

[10.1109/LRA.2020.3015452](https://doi.org/10.1109/LRA.2020.3015452)

Publication date

2020

Document Version

Accepted author manuscript

Published in

IEEE Robotics and Automation Letters

Citation (APA)

Sideris, E. A., De Lange, H. C., & Hunt, A. (2020). An Ionic Polymer Metal Composite (IPMC)-Driven Linear Peristaltic Microfluidic Pump. *IEEE Robotics and Automation Letters*, 5(4), 6788-6795.
<https://doi.org/10.1109/LRA.2020.3015452>

Important note

To cite this publication, please use the final published version (if applicable).
Please check the document version above.

Copyright

Other than for strictly personal use, it is not permitted to download, forward or distribute the text or part of it, without the consent of the author(s) and/or copyright holder(s), unless the work is under an open content license such as Creative Commons.

Takedown policy

Please contact us and provide details if you believe this document breaches copyrights.
We will remove access to the work immediately and investigate your claim.

An Ionic Polymer Metal Composite (IPMC)-Driven Linear Peristaltic Microfluidic Pump

Eva A. Sideris¹, Hendrik C. de Lange¹ and Andres Hunt²

Abstract—Microfluidic devices and micro-pumps are increasingly necessitated in many fields ranging from untethered soft robots, to pharmaceutical and biomedical technology. While realization of such devices is limited by miniaturization constraints of conventional actuators, these restrictions can be resolved by using smart material transducers instead. This paper proposes and investigates the first ionic polymer metal composite (IPMC) actuator-driven linear peristaltic pump. With the aim of designing a monolithic device, our concept is based on a single IPMC actuator that is etched on both sides and cut with kirigami-inspired slits by laser ablation. Our pump has a planar configuration, operates with low activation voltages (< 5 V) and is simple to manufacture and thus miniaturize. We build proof-of-principle prototypes of an open and closed design of our proposed pump concept, model the closed design, and evaluate both configurations experimentally. Results show the feasibility of the proposed IPMC-driven pump. Without any optimization, the open pump achieved pumping rates of $669 \text{ pL} \cdot \text{s}^{-1}$, while the closed pump configuration attained a 4.57 Pa pressure buildup and $9.18 \text{ nL} \cdot \text{s}^{-1}$ pumping rate. These results indicate feasibility of the concept and future work will focus on design optimization.

Index Terms—Biomimetics, Ionic Polymer Metal Composite (IPMC), Medical Robots and Systems, Microfluidics, Peristaltic Pump

I. INTRODUCTION

AUTONOMOUS soft-bodied fluid-actuated microrobots require on-board transducers, valves and pumps etc. with the latter being the most challenging part to realize [1], [2]. Besides soft robotics, microfluidic pumps are increasingly required in applications ranging from cooling appliances in microelectronics, to components of light spacecrafts [3]. Large volumes of microfluidic pumps are required as/for drug delivery systems, medical devices and in-vitro diagnostics equipment, many of which must have dimensions in submillimeter scale. It is worth noting that the globally expanding micro-pump market is expected to attain 19.4% growth rate in 2023 [4].

Peristaltic pumps, both linear and rotary, are currently used in the pharmaceutical, chemical, food and medical industries for example as pumps for handling blood [5]. Furthermore,

they are of interest, due to their biomimicry, in the field of robotics for applications such as urethral sphincters and esophageal swallowing robots [6], [7]. The operation of these pumps is based on the principle of peristalsis: the progressive wavelike contractions and expansions of the walls of hollow organs like in the human's esophagus, stomach and intestines [8]. Working fluids are damaged minimally, since no other moving parts are entailed apart from their mobile pump wall, and contamination can be avoided with disposable pumping chambers [5].

Thus far, peristaltic pumps in the market, i.e. blood pumps for dialysis machines, have only been operated by conventional actuators [9]. Utilization of such pumps in micro-scale applications has been limited due to miniaturization boundaries of conventional actuators [10]. Hence, it is particularly beneficial to introduce smart material actuators as driving mechanisms in micro-pumps [11]. Electromechanical smart material actuators can directly transduce electrical energy to mechanical without the need of bulky ancillary components [12]. They are simple in construction, light-weight and compliant, allowing the realization of simple, light, damage-tolerant structures [13]. Furthermore, smart material transducers can be used to construct entire monolithic mechatronic systems, containing a high count and density of individual actuation units [14], addressed as distributed actuators.

The first pump operated by electromechanical smart materials was published in 1975 by Thomas and Bessman [15]. Since then, electromechanical smart materials have been proposed and investigated for a multitude of microfluidic and micro-pump designs that can mainly be categorized into membrane pumps and linear peristaltic pumps [16].

The reported membrane pumps have been driven by piezoelectric ceramic (PEC) [17], [18], dielectric elastomer (DE) [19] and ferroelectric polymer (FEP) [20], [21] actuators, all of which however require high excitation voltages (100 V up to kV range). Some studies have also used low-voltage smart material actuators (up to 10 V range), i.e. unidirectional shape memory alloy (U-SMA) [22], [23], ionic polymer metal composite (IPMC) [24], [25] and conducting polymer (CP) [26] actuators. While membrane pumps can be realized in compact and miniaturizable structures, they typically require well-defined pump chambers with inlet and outlet mechanisms. Peristaltic pumps do not require any extra parts, rendering them easier to construct compared to membrane pumps.

Various studies have investigated linear peristaltic pumps on the macro-scale using high voltage actuators like DEs [27]–[29]. Potentially miniaturizable linear peristaltic microfluidic pumps have been reported only in very few studies. Their

Manuscript received: February 24, 2020; Revised May 31, 2020; Accepted July 16, 2020.

This paper was recommended for publication by Cecilia Laschi upon evaluation of the Associate Editor and Reviewers' comments.

¹Eva A. Sideris and Hendrik C. de Lange are with Department of Mechanical Engineering, Eindhoven University of Technology, The Netherlands e.a.sideris@tue.nl, h.c.d.lange@tue.nl

²Andres Hunt is with Department of Precision and Microsystems Engineering, Delft University of Technology, The Netherlands a.hunt-1@tudelft.nl

Digital Object Identifier (DOI): see top of this page.

driving mechanisms are based on U-SMA [30], [31], DE [32] and CP [33] actuators. In [30] and in [31], U-SMA wire actuators are used to compress and expand soft tubes. The bases of these pumps support the tubes and additionally facilitate U-SMA cooling and thus permit higher bandwidths. In [28], miniaturization of the DE-actuated self-sealing planar pump of [27] is addressed however, still requiring high actuation voltages. In [33], a linear peristaltic pump design is proposed that consists of a rigid metal core, and a tubular CP actuator that pumps fluid by radially contracting and expanding.

Introduction of low-voltage electromechanical smart material transducers can provide significant advantages to miniature peristaltic pump technology [34]. Although IPMCs have been implemented, as aforementioned, in microfluidic membrane pumps, their viability for operating linear peristaltic pumps has thus far only been theorized in [35], but has never been explored any further. IPMCs are promising candidates for micro-scale applications [24] since they require low voltages (up to 5 V) and exhibit large, bi-directional deflections as well as biocompatibility.

This paper introduces the first IPMC-operated linear peristaltic pump for microfluidic applications. Our pump concept is based on a monolithic IPMC actuator that consists of eight individual actuation elements, following the distributed actuation concept of [14]. First, an IPMC actuator with Na⁺ mobile ions is produced by chemically plating Nafion with platinum (Pt) electrodes. Next, it is processed by laser; to decouple individual actuation units electrically, it is etched on both sides, and to separate them mechanically, it is cut with stress-relief slits which are inspired by kirigami, the art of cutting and folding paper. The resulting actuator is coupled to a clamping system to implement two designs, an open and a closed one. The open pump configuration propels a thin layer of water above the IPMC actuator. The closed pump design includes an elastomeric core that contains the pumped water.

The current paper continues as follows: Section II details IPMC smart materials and their manufacturing and processing to attain the distributed IPMC actuator of our pump concept. Moreover, it further explains the proposed pump designs and proposes a model for the closed pump configuration. Section III explains how both designs are experimentally evaluated, characterizes the pumping performances and discusses the results. The paper is concluded in Section IV.

II. MATERIALS AND METHODS

A. IPMCs

IPMCs are smart materials that exhibit electromechanical as well as mechano-electrical transduction i.e. actuating and sensing [36]. They are thin (typically about 0.2 mm thick) tri-layer composites that consist of two metal electrodes and an ionomer layer in between, traditionally, Pt (each electrode is usually roughly 0.01 mm thick) and Nafion (commonly 0.18 mm thick) respectively [36]–[38]. IPMCs normally work hydrated with water or saturated with liquid salts [36], [37]. The latter can operate for long periods in air as liquid salts are not volatile [36] while the former require aqueous environments for long-term operation to avoid water evaporation [37].

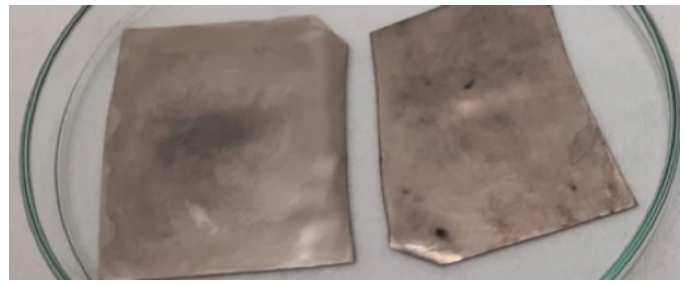


Fig. 1. Manufactured sheets of IPMC actuators.

During actuation bending commences due to ion migration that occurs when applying a potential difference to the electrodes [36]. The bending direction can be altered by alternating the voltage polarity.

B. IPMC Manufacturing

Nafion-based IPMCs with Pt electrodes and Na⁺ counterions are utilized in this study (Fig. 1). These are fabricated in-house with the chemical plating method of impregnation-reduction, with a similar methodology as reported in [38], [39]. Initially, the surface of a commercial NafionTM117 membrane (Alfa Aesar), with a thickness of 0.18 mm, is roughened with a fine grit size sandpaper (ISO P1000) to increase the membrane's surface area. Residues are subsequently removed from the film by cleaning in an ultrasonic bath and boiling in 2.4 M HCl and then water. The membrane is afterwards impregnated with Pt particles by immersing in a [Pt(NH₃)₄]Cl₂ complex (Sigma Aldrich) solution for over 10 hours. Primary plating commences with reducing the impregnated Pt complex ions into metal nanoparticles by adding NaBH₄ (Sigma Aldrich) while heating the mixture to 60°C. Secondary plating ensues by growing the already deposited Pt layer by placing the membrane into aqueous [Pt(NH₃)₄]Cl₂ and NH₄OH solution, and slowly heating the solution to 60°C, while incrementally adding H₂NOH·HCl and NH₂NH₂·H₂O over the period of 4 hours. The material is finally protonated in 0.1 M HCl solution, and ion-exchanged in 0.1 M NaOH solution, resulting in Na⁺ mobile ion-containing IPMCs.

C. IPMC Processing

An Optec WS-STARTER laser micro-machining system, with a theoretical laser focus spot of 7 μm, is used to etch both sides and cut the IPMC actuator. Laser parameters (i.e. repetitions, laser speed, firing rate etc.) for the etching and cutting depend highly on particular sample properties and hydration, and are established experimentally for each specimen. For etching away the IPMC electrodes, the best results were achieved with 30 repetitions at 10 μm steps, using a laser speed of 5000 mm · s⁻¹, at 100 kHz firing rate. For cutting, the best results were achieved when repeating 30 times at 200 mm · s⁻¹ speed and 250 kHz laser firing.

Before designing the pump's distributed IPMC actuator, it is necessary to determine the pattern of the mechanical stress-relief slits of the etched areas, which have a thickness of approximately 0.18 mm, between the individual actuation

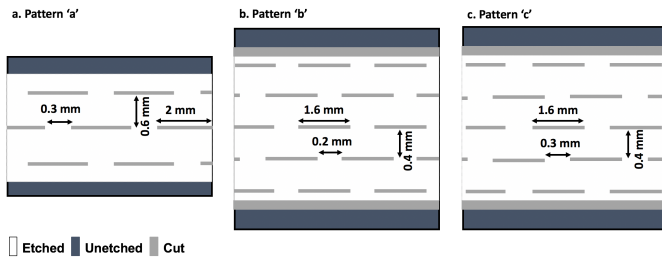


Fig. 2. Investigation of 3- and 5-line kirigami-inspired patterns 'a', 'b' and 'c' for the distributed IPMC actuator's stress-relief cuts. Etched areas are represented in white. Unetched parts are colored in dark grey and cut regions are in light grey.

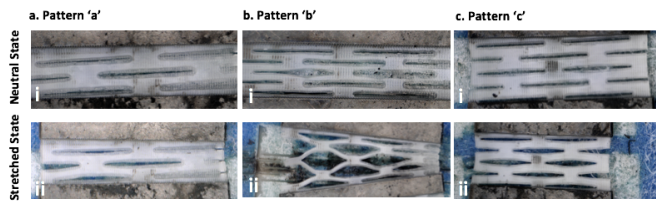


Fig. 3. Microscopic testing of the 3- and 5-line kirigami-inspired patterns 'a', 'b' and 'c' in their neutral state (first row) and stretched state (second row).

units that are about 0.2 mm thick. The pattern is characterized by the number of parallel lines and their lengths, and the distance between collinear lines and parallel lines. The slits should enable the distributed actuator to remain mechanically intact and allow the actuation units sufficient mobility. Our initial pattern 'a' (Fig. 2a and Fig. 3ai) was implemented and subsequently evaluated in its stretched configuration (Fig. 3aii), using a Keyence VHX-6000 optical microscope. Since the pattern did not provide sufficient mobility, we therefore tested a variation, pattern 'b' (Fig. 2b and Fig. 3bi), which however failed to provide structural integrity (Fig. 3bii). Hence, we experimented further with pattern 'c' (Fig. 2c and Fig. 3ci), which did provide the structural integrity and mobility required (Fig. 3cii) and was consequently selected for our distributed actuator design (see Section II-D). Patterns 'a', 'b' and 'c' were all conducted on the same IPMC sample to avoid variations in properties between different specimens. We observed that implementing these patterns is a trade-off between not cutting through the Nafion ionomer and causing heat damage.

D. Distributed IPMC Actuator

Our pump's driving solution (Fig. 4 and Fig. 5), is a 20.1 mm x 19 mm distributed IPMC actuator that consists of eight actuation elements. These operate in four pairs and have widths of 4 mm, free lengths of 6.8 mm, and 4 mm x 2 mm clamping areas at their bases.

The actuator is produced by processing a single IPMC sample with a pulsed laser system. 1.4 mm wide portions of the IPMC's Pt electrodes are etched away on both sides to provide electrical insulation between the individual actuation elements. Furthermore, the IPMC is also cut to provide mechanical decoupling to the actuation units and coupling to

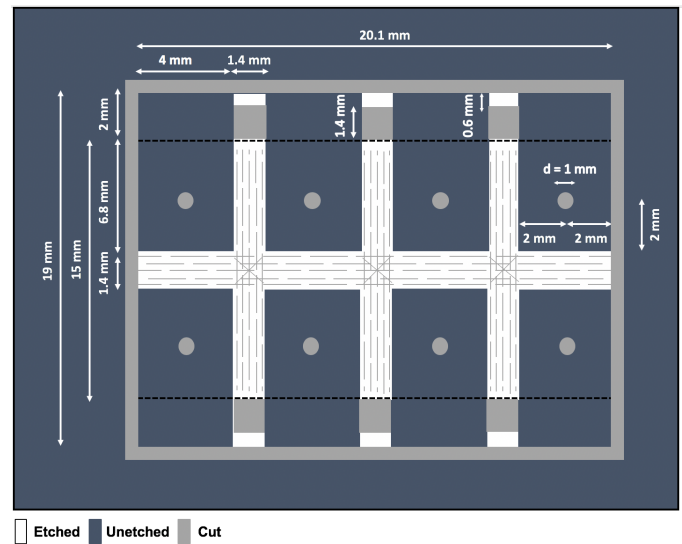


Fig. 4. Design of the distributed IPMC actuator of our linear peristaltic microfluidic pump concept (top view). It is created by etching both sides and then cutting a single IPMC. Etched areas are represented in white. Unetched parts are colored in dark grey and cut regions in light grey.

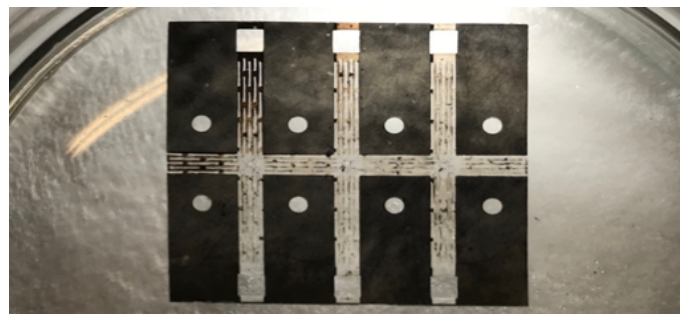


Fig. 5. Photograph of distributed IPMC actuator that drives our linear peristaltic microfluidic pump.

ancillary pump parts. The former is attained by implementing the selected kirigami-inspired stress-relief cuts (see Section II-C) which are oriented parallel to the sides of the actuation elements. Additional 'X' slits are also introduced at the intersections of the decoupling patterns to decouple stresses in the horizontal and vertical direction. Square locking holes, 1.4 mm in side-lengths, are also cut in between the elements' clamping areas to secure the actuator to the clamping system via the guiding pins of the latter (see Section II-E). Moreover, for the closed pump design, circular locking holes of 1 mm in diameter are cut in the center of each element to attach the actuator to the protruding locking pins of the pump's silicone core (see Section II-E).

E. Open and Closed Pump Designs

Our pump concept is based on coupling the distributed IPMC actuator to a 3D-printed spring-loaded clamping system (PLA plastic, Ultimaker 3) (Fig. 6). The latter provides mechanical fixation to the IPMC which is aligned through locking holes with the clamping system's built-in guiding pins. Moreover, the clamping system also contains 16 gold (Au) electrodes and respective wiring for connecting each actuation

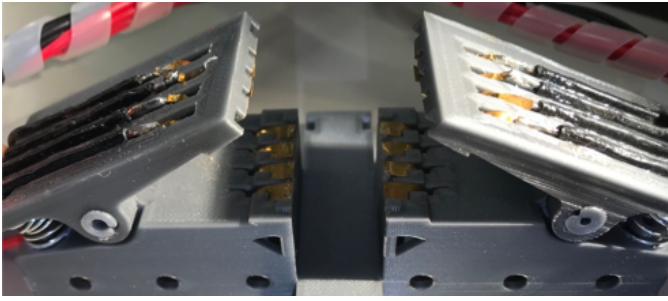


Fig. 6. Clamping system that provides mechanical support and electrical connections to the actuation units of the distributed IPMC actuator driving our proposed linear peristaltic pump.



Fig. 7. Assembled open pump design with distributed IPMC actuator coupled to the clamping system.

unit to an amplifier. Au is selected as it is electrochemically inert, therefore preventing contamination of the IPMC actuator.

We evaluate two pump designs that utilize the same distributed IPMC actuator and clamping system. Initially, we investigate an open pump design (Fig. 7) where the distributed IPMC actuator is connected to the clamping system and a thin layer of water of 0.89 mm covers the actuator. The actuator's peristaltic motion propels the liquid layer from one end to the other. Next, we examine a closed pump design, where the pumped water is contained in an elastomeric core. The core (Fig. 8) consists of a silicone membrane (Smooth-On Ecoflex 00-10) which is supported on a 3D-printed backbone (PLA plastic, Ultimaker 3) and has eight 3D-printed spikes (ABS plastic, Envisiontec Micro HiRes Plus) attached, for coupling with the IPMC actuation units. The membrane was cast in a mold which contained the backbone and the spikes were thereafter added with the aid of an alignment grid before curing the silicone for 4h. Subsequently, the membrane is fixed with axillary parts on a 3D-printed substrate (PLA plastic, Ultimaker 3) which also contains the pump's inlet and outlet fluid channels. Finally, the distributed IPMC actuator is connected to the core prior to coupling to the clamping system (Fig. 9).

F. Closed Pump Design Model

The model of a linear peristaltic pump depends on its design, and may require consideration of inertial and viscous forces, mixing of fluids, and other effects [40]–[43]. For the proposed closed pump design we derive a kinematic model that describes the performance of an ideal pump and we further introduce leakage terms in order to model our final prototype. This model does not describe the open pump design as in this case the pump's operation is governed by viscous forces.

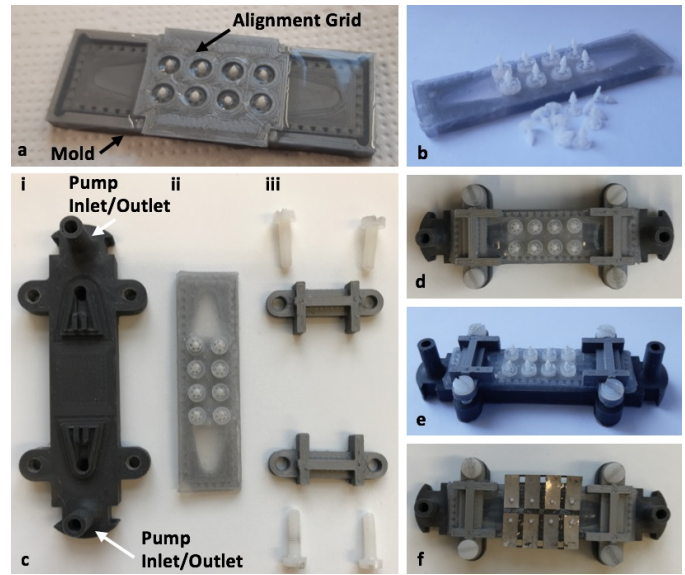


Fig. 8. Core for closed pump design. a. Manufacturing of core's membrane (silicone curing), b. Membrane supported on 3D-printed backbone and integrated with eight 3D-printed spikes (silicone cured, mold and alignment grid removed), c. Individual core parts: ci. 3D-printed substrate, cii. Membrane, ciii. Axillary fixing parts, d. Assembled core (topview), e. Assembled core (side-view), f. Distributed IPMC actuator attached to core by its pins.



Fig. 9. Assembled closed pump design with core and distributed IPMC actuator positioned in the clamping system.

The proposed planar linear peristaltic pump design is illustrated in Fig. 10. Since the IPMC actuators apply bipolar displacements, the pump's membrane is raised from the rigid substrate by a distance a . Under sinusoidal excitation with amplitude b , wavelength λ and wave propagation speed c , the membrane height A in the pump's symmetry plane can be described similarly to the urethra model in [40]:

$$A(x, t) = \left\{ a + b \cdot \sin \left[\frac{2\pi}{\lambda} \cdot (x + ct) \right] \right\}^+ \quad (1)$$

where x is the coordinate in the pumping direction and t is time. Please note that only positive membrane heights are admissible. The height of the membrane over the cross-section

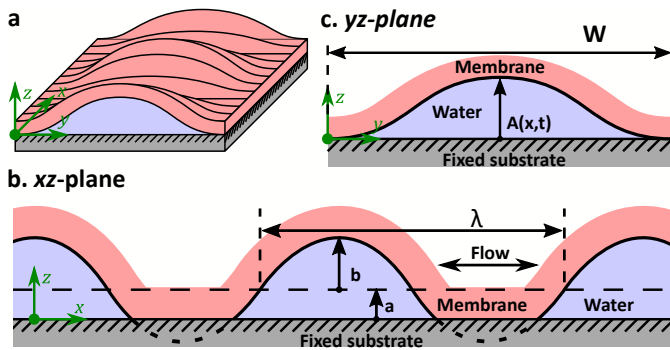


Fig. 10. Planar linear peristaltic pump in actuated state. a. Perspective view, b. Cross-sectional-view, c. Lengthwise-view in the pump's plane of symmetry.

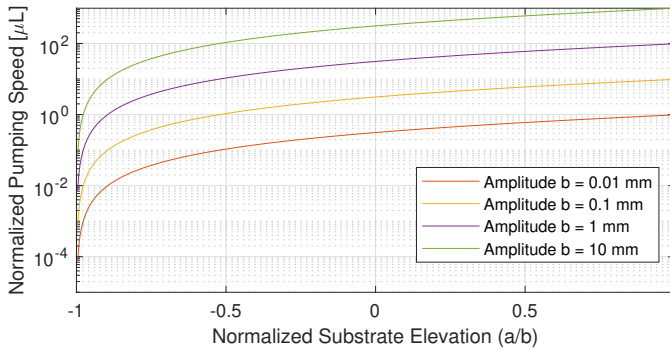


Fig. 11. Pumping rates of an ideal linear peristaltic pump. Pumping rates are normalized with respect to the pumping frequency ν (thus the unit $\mu\text{L} \cdot \text{s}^{-1} \cdot \text{Hz}^{-1} = \mu\text{L}$). Substrate elevations b are normalized with respect to the pumping amplitude. Calculations use $\lambda = 3/4L$ and $W = 13 \text{ mm}$, as in our closed pump prototype. See Fig. 10 for notation.

of the pump that has a width of W can be written as:

$$h(x, y, t) = 0.5 \cdot A(x, t) \cdot \left(1 - \cos\left(\frac{2\pi y}{W}\right)\right) \quad (2)$$

where y is the coordinate in the width direction. Next we can express the area of pump's cross-section as:

$$CS(x, t) = \int_0^W h(x, y, t) dy = 0.5 W \cdot A(x, t) \quad (3)$$

the fluid volume that is contained in a single wavelength as:

$$V_\lambda = 0.5 W \cdot \int_0^\lambda A(x, t) dx \quad (4)$$

and the average pumping speed for excitation frequency ν as:

$$\frac{dV}{dt} = V_\lambda \nu \quad (5)$$

This kinematic model is valid for $|a| < b$. The maximum wavelength volume $V_{\lambda \max} = 0.5W$ is achieved when $a = b$. This model allows for evaluation of the performance of an ideal pump, as shown for various actuation amplitudes in Fig. 11.

In practice, the pumping performance is affected by many additional factors, e.g. the compliance, imperfections and dynamics of the IPMC and the membrane. Therefore, V_λ also varies with frequency. To validate our design, our prototype

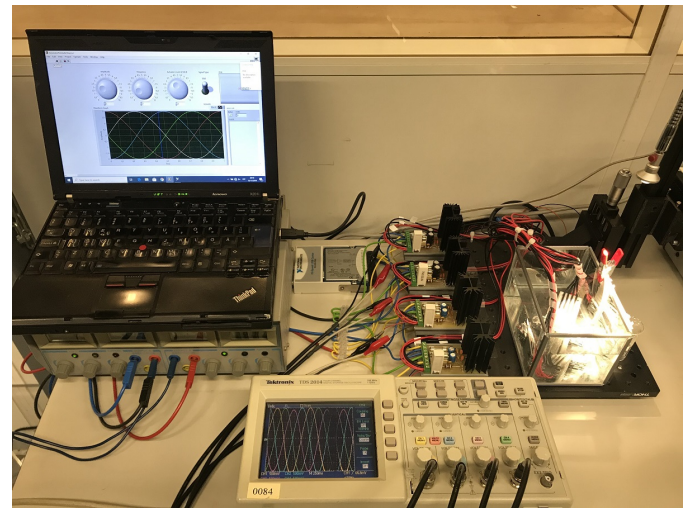


Fig. 12. Experimental set-up for testing the two designs of the IPMC-operated pump concept. The pumps are operated in a water tank to avoid IPMC dehydration during actuation.

pumps fluid from one column to another, building up a pressure difference. This results in back-leakage via the compliant pump membrane. Combining the pumping and leakage effects, the net fluid displacement rate can be described as:

$$\frac{dV_{net}}{dt} = v_p - cV_{net} \quad (6)$$

where $v_p = V_\lambda \nu$ is the pumping speed from (5) and c is a pressure-dependent proportional leakage coefficient (note that pressure is proportional to volume). Equation (6) yields:

$$V_{net} = \frac{v_p t + V_0}{1 + ct} \quad (7)$$

where V_0 is the initial volume. Fluid loss additionally occurs due to imperfect sealing between the component couplings. This out-leakage rate v_{OL} is very slow and can be considered constant. Therefore, the total amount of fluid in the tube can be described as:

$$V_{total} = \frac{v_p t + V_0}{1 + ct} + v_{OL} t \quad (8)$$

This model is further used in experimentally evaluating the pumping characteristics of our closed peristaltic pump prototype.

III. EXPERIMENTAL EVALUATION

To evaluate the pumping functionality of the proposed IPMC-driven linear peristaltic pump designs, we experimentally identify the flow speeds (for open design) and the pressures (for closed design) that they induce in response to different IPMC excitation signals. For this purpose, we construct an experimental set-up consisting of an excitation system and a camera (Fig. 12 and Fig. 13). During the experiments, the pumps are placed in a water tank to prevent IPMC dehydration. Manufacturing and operation of the pump prototypes are shown in the video attachment.

The IPMC actuation units of the distributed actuator are excited in four pairs using four custom-built unity gain buffer

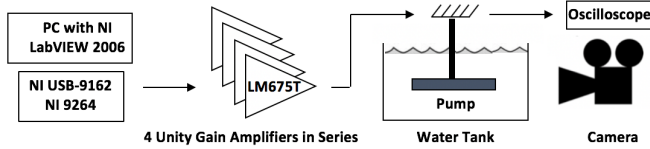


Fig. 13. Block diagram of experimental set-up for testing the IPMC-operated pump concept. The camera is positioned above the water tank for evaluating the open pump design and on the side for the closed design.

TABLE I
RESULTS OF OPEN PUMP DESIGN AT 2 V SINUSOIDAL WAVE.

Phase Difference	Frequency	Pumping speed
120°	0.5 Hz	316 $pL \cdot s^{-1}$
90°	0.5 Hz	669 $pL \cdot s^{-1}$
90°	1 Hz	614 $pL \cdot s^{-1}$
90°	2 Hz	537 $pL \cdot s^{-1}$

amplifiers (LM675T), which are further powered by a power supply (Agilent 33220A). The actuation signals are generated in a PC using National Instruments (NI) LabVIEW 2016 software and are converted from digital to analogue using data acquisition modules (NI USB-9162 and NI 9264). The LabVIEW program drives the actuation unit pairs with sinusoidal waveforms, allowing to specify the frequencies, amplitudes and phase differences between successive actuation pairs. An oscilloscope (Tektronix TDS 2014) validates that our IPMC pairs are receiving the expected excitation inputs.

To characterize the pumping performances, we use a camera (Xiaomi Redmi 5, 1080p) to record the experiments. The videos are post-processed using ImageJ 1.52a software with Manual Tracking plugin to extract the pumping speeds and pressures.

In the experiments of the open pump design, the camera is positioned above the pump. Microparticles are dispersed in the water tank to record their motion above the actuator, allowing to subsequently estimate the working fluid's velocity.

The IPMC actuation units are excited with sinusoidal signals of 2 V in amplitude. While higher voltages induce higher deflections that should therefore also translate into higher pumping speeds, we cannot go beyond 2 V due to hydrolysis that causes disturbances in the fluid flow.

Results (Table I) show that phase differences of 90° between successive actuation units yield higher pumping rates than 120°. For 0.5 Hz these pumping rates are 669 $pL \cdot s^{-1}$ and 316 $pL \cdot s^{-1}$ respectively. Experiments at different frequencies (0.5 Hz to 3 Hz) and 90° phase differences achieve a maximum pumping rate of 669 $pL \cdot s^{-1}$ at 0.5 Hz. This operating point is a tradeoff between the fluid and IPMC actuator dynamics. In future work we expect to attain higher rates by preventing leakage through the cuts of the IPMC.

In the experiments of the closed pump design, the pumped water is separated from the water in the tank (Fig. 14). Transparent vertical tubes are connected to the inlet and outlet of the pump to record the height of the contained working fluid as it is juxtaposed against a millimeter grid reference.

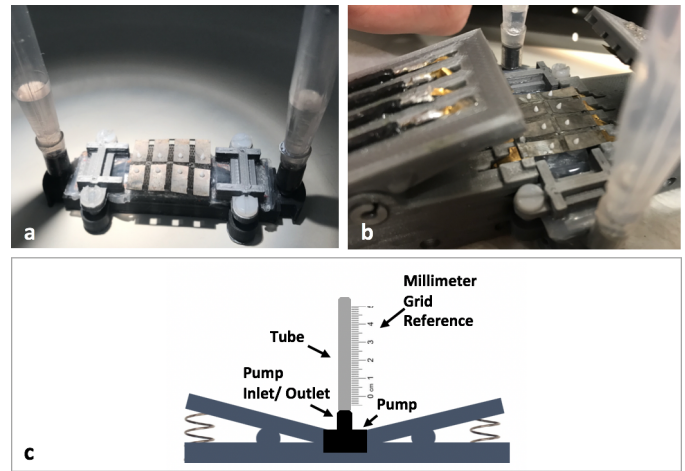


Fig. 14. Evaluation of closed pump design. a. Transparent vertical tubes are connected to pump inlet and outlet and water is added to core, b. Positioning in clamp, c. Side-view.

Generated pressures are thereafter calculated from the water level measurements extracted from the videos.

We first compare the pumping performance at 90° and 120° phase differences between successive actuation units by using sinusoidal excitation signals of 0.5 Hz to 3 Hz at 3.5 V. Results indicate (opposite to the open pump design) that the signal with 120° phase differences achieves a significantly better performance. We therefore repeat individual experiments at 4 V sinusoidal excitation signals with 120° phase differences at 0.5 Hz, 1 Hz and 3 Hz frequencies (Fig. 16). The pump attains a steady-state pumping pressure of 3.66 Pa at 0.1 Hz, 4.57 Pa at 1 Hz and 4.29 Pa at 3 Hz. Next, using these results to fit our model, we identify the pumping rate v_p and back-leakage coefficient c to get $c = 0.383 s^{-1}$ (identical for all experiments) and v_p of 7.36 $nL \cdot s^{-1}$ for 0.5 Hz, 9.18 $nL \cdot s^{-1}$ for 1 Hz and 8.63 $nL \cdot s^{-1}$ for 3 Hz. We observed a slow out-leakage of water from the pump to the tank, caused by imperfections in the sealing between the pump components. We identified its average rate to be 63.8 $pL \cdot s^{-1}$, causing a pressure drop of 12.7 $mPa \cdot s^{-1}$ (indicated as 'leakage' in Fig. 15 and Fig. 16).

As this is the first report on IPMC-driven linear peristaltic pumps, there is no work in the literature to which we can directly compare the results. Compared to IPMC-operated membrane micro-pumps, our best pumping rate of 551 $nL \cdot min^{-1}$ is significantly less than 130 $\mu L \cdot min^{-1}$ achieved by Wang *et al.* [24] or 760 $\mu L \cdot min^{-1}$ by Nguyen *et al.* [25]. Previously reported linear peristaltic pumps driven by other smart materials such as U-SMAs have achieved 230 $\mu L \cdot min^{-1}$ [30] and CPs have attained 2.5 $\mu L \cdot min^{-1}$ [33].

This clearly indicates that our design requires optimization, which will be our main objective in future work. We hypothesize that the main issue lies in the transformation of power from the IPMC actuator to the pumping of the fluid. We expect to improve efficiency significantly by simplifying the design through integrating the membrane with the IPMC actuator (simplifying the IPMC - membrane coupling), adding more

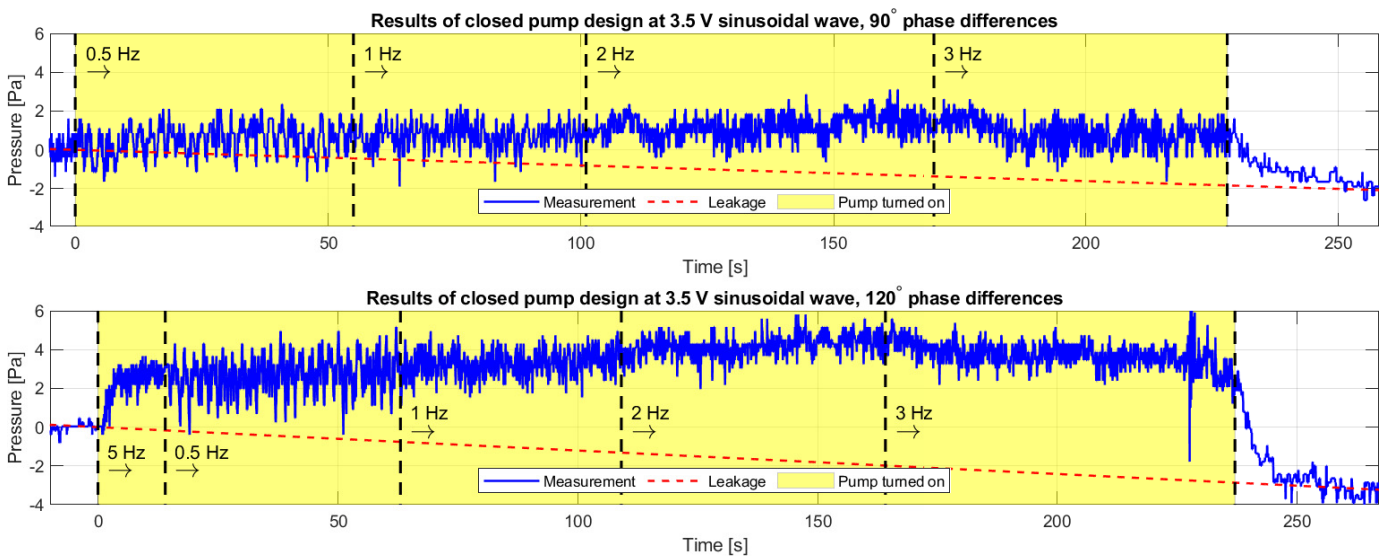


Fig. 15. Experimentally measured pumping pressures of the closed pump design for sinusoidal excitation signals at 90° (top) and 120° (bottom) phase differences at 3.5 V amplitude. Frequencies of 0.5 Hz , 1 Hz , 2 Hz and 3 Hz are applied sequentially. Out-leakage of the working fluid is indicated with the red dashed lines.

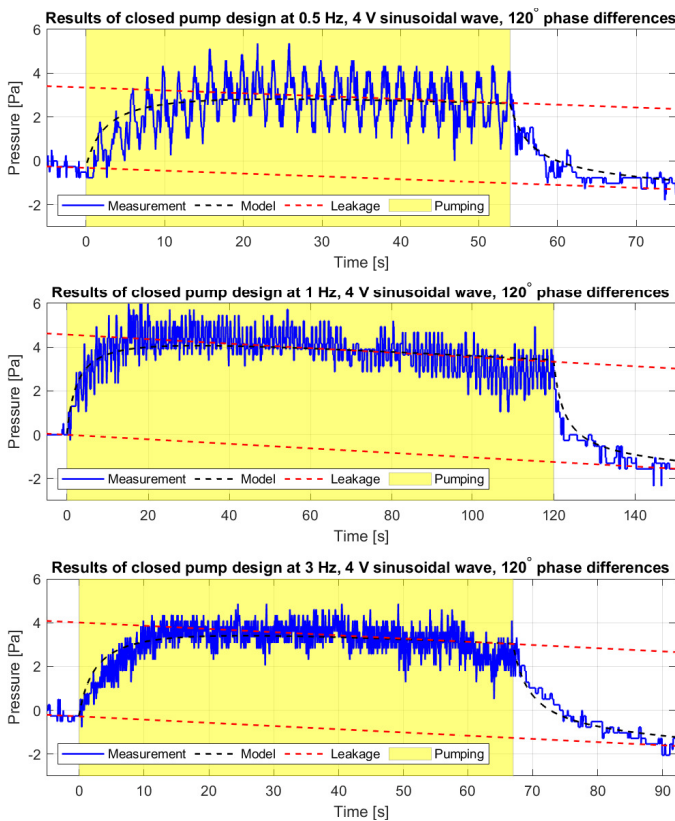


Fig. 16. Experimentally obtained pressure differences of the closed pump prototype: at 0.5 Hz (top), 1 Hz (middle) and 3 Hz (bottom) (4 V amplitude). Plots show the measured results (blue), the leakage of working fluid (dashed red) and the modeled results (dashed black).

actuation units in series (giving higher actuation resolution) and optimizing dimensions in COMSOL software. Simplifying the design should also result in a much more miniaturizable pump.

IV. CONCLUSION

Simple and miniaturizable pumps are increasingly required for integration in future microfluidic applications ranging from soft robots, micro-electronics and spacecrafts, to drug delivery and medical devices and in-vitro diagnostics. Miniaturization constraints of conventional transducers can be overcome by using smart material actuators. This work proposes the first IPMC-driven peristaltic pump for future microfluidic applications. It first proposes and builds proof-of-concept prototypes of an open and closed pump design, models the latter, and further evaluates the pumping performances of both configurations experimentally. The proposed pump is operated by a distributed IPMC actuator with a $20.1\text{ mm} \times 19\text{ mm}$ footprint. It comprises a monolithic structure that contains eight individual actuation units and is created by etching and cutting a single IPMC actuator with laser micromachining methods. Results for the open pump design showed a maximum pumping rate of $669\text{ pL} \cdot \text{s}^{-1}$ when excited at 0.5 Hz , 2 V amplitude, using 90° phase differences between successive actuation units. The closed pump achieved a pumping rate of $9.18\text{ nL} \cdot \text{s}^{-1}$ and a steady-state pressure of 4.57 Pa when excited at 1 Hz , 3.5 V amplitude, using 120° phase differences. All in all, this work proposes and demonstrates pumping functionality of the first IPMC-driven peristaltic pump. In future work we will optimize its design to improve efficiency and down-scaling.

REFERENCES

- [1] C. Cao, X. Gao, and A. T. Conn, "A magnetically coupled dielectric elastomer pump for soft robotics," *Advanced Materials Technologies*, vol. 4, no. 8, p. 1900128, 2019.

- [2] V. Cacucciolo, J. Shintake, Y. Kuwajima, S. Maeda, D. Floreano, and H. Shea, "Stretchable pumps for soft machines," *Nature*, vol. 572, no. 7770, pp. 516–519, 2019.
- [3] D. J. Laser and J. G. Santiago, "A review of micropumps," *Journal of micromechanics and microengineering*, vol. 14, no. 6, p. R35, 2004.
- [4] The Editors of Market Research Future. Micro pump market research report - global forecast till 2023. [Online]. Available: <https://www.marketresearchfuture.com/reports/micro-pump-market-1300>
- [5] M. Stewart, *Surface Production Operations: Volume IV: Pumps and Compressors*. Gulf Professional Publishing, 2018.
- [6] F. Chen, S. Dirven, W. Xu, and X. Li, "Soft actuator mimicking human esophageal peristalsis for a swallowing robot," *IEEE/ASME Transactions on Mechatronics*, vol. 19, no. 4, pp. 1300–1308, 2013.
- [7] M. Cianchetti, C. Laschi, A. Menciassi, and P. Dario, "Biomedical applications of soft robotics," *Nature Reviews Materials*, vol. 3, no. 6, pp. 143–153, 2018.
- [8] The Editors of Encyclopaedia Britannica. (2019, Sept.) Peristalsis. [Online]. Available: <https://www.britannica.com/science/peristalsis>
- [9] W. Hörnl, K. Koch, R. Lindsay, C. Ronco, and J. Winchester, *Replacement of renal function by dialysis*. Springer, 2004.
- [10] A. B. Neto, A. Lima, H. Neff, C. L. Gomes, and C. Moreira, "Linear peristaltic pump driven by three magnetic actuators: Simulation and experimental results," in *2011 IEEE International Instrumentation and Measurement Technology Conference*. IEEE, 2011, pp. 1–6.
- [11] R. Samatham, K. Kim, D. Dogruer, H. Choi, M. Konyo, J. Madden, Y. Nakabo, J.-D. Nam, J. Su, S. Tadokoro, et al., "Active polymers: an overview," in *Electroactive polymers for robotic applications*. Springer, 2007, pp. 1–36.
- [12] W. MohdIsa, A. Hunt, and S. H. HosseinNia, "Sensing and self-sensing actuation methods for ionic polymer–metal composite (ipmc): A review," *Sensors*, vol. 19, no. 18, p. 3967, 2019.
- [13] J. D. Madden, N. A. Vandesteeg, P. A. Anquetil, P. G. Madden, A. Takshi, R. Z. Pytel, S. R. Lafontaine, P. A. Wieringa, and I. W. Hunter, "Artificial muscle technology: physical principles and naval prospects," *IEEE Journal of oceanic engineering*, vol. 29, no. 3, pp. 706–728, 2004.
- [14] A. Hunt, M. Freriks, L. Sasso, P. M. Esfahani, and S. H. HosseinNia, "Ipmc kirigami: A distributed actuation concept," in *2018 International Conference on Manipulation, Automation and Robotics at Small Scales (MARSS)*. IEEE, 2018, pp. 1–6.
- [15] L. Thomas Jr and S. Bessman, "Prototype for an implantable micropump powdered by piezoelectric disk benders," *Transactions-American Society for Artificial Internal Organs*, vol. 21, pp. 516–522, 1975.
- [16] E. Sideris and H. de Lange, "Pumps operated by solid-state electromechanical smart material actuators—a review," *Sensors and Actuators A: Physical*, p. 111915, 2020.
- [17] A. Choi, S. L. Vatanabe, C. R. de Lima, and E. C. Silva, "Computational and experimental characterization of a low-cost piezoelectric valveless diaphragm pump," *Journal of intelligent material systems and structures*, vol. 23, no. 1, pp. 53–63, 2012.
- [18] M. Koch, A. Evans, and A. Brunnschweiler, "The dynamic micropump driven with a screen printed pzt actuator," *Journal of Micromechanics and Microengineering*, vol. 8, no. 2, p. 119, 1998.
- [19] F. A. M. Ghazali, C. K. Mah, A. AbuZaiter, P. S. Chee, and M. S. M. Ali, "Soft dielectric elastomer actuator micropump," *Sensors and Actuators A: Physical*, vol. 263, pp. 276–284, 2017.
- [20] Y. Kim, J. Kim, K. Na, and K. Rhee, "Experimental and numerical studies on the performance of a polydimethylsiloxane valveless micropump," *Proceedings of the Institution of Mechanical Engineers, Part C: Journal of Mechanical Engineering Science*, vol. 219, no. 10, pp. 1139–1145, 2005.
- [21] F. Xia, S. Tadigadapa, and Q. Zhang, "Electroactive polymer based microfluidic pump," *Sensors and Actuators A: Physical*, vol. 125, no. 2, pp. 346–352, 2006.
- [22] W. L. Benard, H. Kahn, A. H. Heuer, and M. A. Huff, "Thin-film shape-memory alloy actuated micropumps," *Journal of Microelectromechanical systems*, vol. 7, no. 2, pp. 245–251, 1998.
- [23] D. Xu, L. Wang, G. Ding, Y. Zhou, A. Yu, and B. Cai, "Characteristics and fabrication of niti/si diaphragm micropump," *Sensors and Actuators A: Physical*, vol. 93, no. 1, pp. 87–92, 2001.
- [24] J. Wang, A. McDaid, R. Sharma, W. Yu, and K. C. Aw, "Miniature pump with ionic polymer metal composite actuator for drug delivery," in *Ionic Polymer Metal Composites (IPMCs)*, 2015, pp. 19–45.
- [25] T. T. Nguyen, V. K. Nguyen, Y. Yoo, and N. S. Goo, "A novel polymeric micropump based on a multilayered ionic polymer-metal composite," in *IECON 2006-32nd Annual Conference on IEEE Industrial Electronics*. IEEE, 2006, pp. 4888–4893.
- [26] J. H. Kim, K. T. Lau, and D. Diamond, "Fabrication of microfluidic pump using conducting polymer actuator," in *2008 IEEE International Conference on Sensor Networks, Ubiquitous, and Trustworthy Computing (suc 2008)*. IEEE, 2008, pp. 457–463.
- [27] P. Lotz, M. Matysek, and H. F. Schlaak, "Peristaltic pump made of dielectric elastomer actuators," in *Electroactive Polymer Actuators and Devices (EAPAD) 2009*, vol. 7287. International Society for Optics and Photonics, 2009, p. 72872D.
- [28] F. Carpi, C. Menon, and D. De Rossi, "Electroactive elastomeric actuator for all-polymer linear peristaltic pumps," *IEEE/ASME Transactions on mechatronics*, vol. 15, no. 3, pp. 460–470, 2009.
- [29] X. Wu, W. Sun, B. Li, H. Chen, and J. Zhou, "Homogeneous large deformation analysis of a dielectric elastomer peristaltic actuator," *Science China Technological Sciences*, vol. 55, no. 2, pp. 537–541, 2012.
- [30] S. K. Sagar and M. Sree Kumar, "Miniaturized flexible flow pump using sma actuator," *Procedia Engineering*, vol. 64, pp. 896–906, 2013.
- [31] E. Borlandelli, D. Scarselli, A. Nespoli, D. Rigamonti, P. Bettini, M. Morandini, E. Villa, G. Sala, and M. Quadrio, "Design and experimental characterization of a niti-based, high-frequency, centripetal peristaltic actuator," *Smart materials and structures*, vol. 24, no. 3, p. 035008, 2015.
- [32] S. Solano-Arana, F. Klug, H. Mößinger, F. Förster-Zügel, and H. F. Schlaak, "A novel application of dielectric stack actuators: a pumping micromixer," *Smart Materials and Structures*, vol. 27, no. 7, p. 074008, 2018.
- [33] Y. Wu, D. Zhou, G. M. Spinks, P. C. Innis, W. Megill, and G. Wallace, "Titan: a conducting polymer based microfluidic pump," *Smart materials and structures*, vol. 14, no. 6, p. 1511, 2005.
- [34] F. Amirouche, Y. Zhou, and T. Johnson, "Current micropump technologies and their biomedical applications," *Microsystem technologies*, vol. 15, no. 5, pp. 647–666, 2009.
- [35] S. Vohnout, S.-M. Kim, I.-S. Park, M. Banister, R. Tiwari, and K. J. Kim, "Ipmc-assisted miniature disposable infusion pumps with embedded computer control," in *Electroactive Polymer Actuators and Devices (EAPAD) 2007*, vol. 6524. International Society for Optics and Photonics, 2007, p. 65241U.
- [36] M. Shahinpoor, *Ionic Polymer Metal Composites (IPMCs): Smart Multi-Functional Materials and Artificial Muscles Volume 2*. Royal Society of Chemistry, 2015.
- [37] M. Shahinpoor, Y. Bar-Cohen, J. Simpson, and J. Smith, "Ionic polymer-metal composites (ipmcs) as biomimetic sensors, actuators and artificial muscles—a review," *Smart materials and structures*, vol. 7, no. 6, p. R15, 1998.
- [38] K. J. Kim and M. Shahinpoor, "Ionic polymer–metal composites: II. manufacturing techniques," *Smart materials and structures*, vol. 12, no. 1, p. 65, 2003.
- [39] V. De Luca, P. Digiambardino, G. Di Pasquale, S. Graziani, A. Pollicino, E. Umana, and M. G. Xibilia, "Ionic electroactive polymer metal composites: fabricating, modeling, and applications of postsilicon smart devices," *Journal of Polymer Science Part B: Polymer Physics*, vol. 51, no. 9, pp. 699–734, 2013.
- [40] T. W. Latham, "Fluid motions in a peristaltic pump." Ph.D. dissertation, Massachusetts Institute of Technology, 1966.
- [41] N. Elabbasi, J. Bergstrom, and S. Brown, "Fluid-structure interaction analysis of a peristaltic pump," in *COMSOL conference in Boston*, 2011.
- [42] Y. Bar-Cohen and Z. Chang, "Piezoelectrically actuated miniature peristaltic pump," in *Smart Structures and Materials 2000: Active Materials: Behavior and Mechanics*, vol. 3992. International Society for Optics and Photonics, 2000, pp. 669–676.
- [43] N. Nguyen and X. Huang, "Miniature valveless pumps based on printed circuit board technique," *Sensors and Actuators A: Physical*, vol. 88, no. 2, pp. 104–111, 2001.